A new class of nonseparable and nonstationary covariance models for wind fields[1]

Montserrat Fuentes, Li Chen, Jerry M. Davis, and Gary Lackmann

SUMMARY

Classical geostatistical methods are powerful tools to study the spatial-temporal structure of stationary processes. Separability is also a common assumption to avoid many of the problems of space and time modeling. This subclass of separable spatial-temporal processes has several advantages, including rapid fitting and simple extensions of many techniques developed and successfully used in time series analyses and geostatistics. However, in real applications spatial-temporal processes are rarely stationary and separable; then an important extension of these traditional geostatistical methods is to processes that have a nonstationary and nonseparable covariance. In this work, some new approaches to estimate and model nonstationarity and nonseparability are presented. The most important scientific contributions of the research proposed here are; the estimation of the complex spatial-temporal dependence of environmental processes in general situations (nonstationarity, anisotropy, nonseparability), and the introduction of flexible models for spatial prediction of environmental processes. We apply the statistical methods proposed here to model the spatial-temporal patterns of wind fields, and for wind field mapping, which combines numerical meteorological model output with observational data. The data used in this phase of the research came from the subregion surrounding and including the Chesapeake Bay for July 2002. The ability to accurately forecast wind speed and direction in coastal locations is critical for support of shipping, marine recreational activities, and national security issues related to contaminant transport.

[1]M. Fuentes is an associate professor at the Statistics Department, North Carolina State University (NCSU), Raleigh, NC 27695-8203, and a visiting scientist at the US Environmental Protection Agency (EPA). Tel.:(919) 515-1921, Fax: (919) 515-1169, E-mail: fuentes@stat.ncsu.edu. L. Chen is a graduate student in the Statistics Department at NCSU. J. Davis is a professor in the Marine Earth and Atmospheric Sciences Department at NCSU. G. Lackmann is an assistant professor in the Marine Earth and Atmospheric Sciences Department at NCSU. This research was sponsored by a National Science Foundation grant DMS 0002790, and by a U.S. Defense Threat Reduction Agency (DTRA) grant.

Key words: Bayesian inference, Fourier transform, geostatistics, meteorological mesoscale model (MM5), nonseparable models, nonstationary models, wind fields.

1 Introduction

Increased emphasis on homeland security issues provides an additional incentive for developing accurate meteorological analysis and forecast fields for the coastal wind regime. The transport of chemical or biological agents is critically dependent on accurate forecasts of meteorological fields such as the near-surface wind speed and direction. These forcasts in turn depend on the accuracy of the observed data fields that go into the numerical meteorological model which produces these forecasts. The emphasis in this paper will be on the development of a procedure that could potentially be used to improve either the assimilation of surface wind observations into a model initial field, or to improve the accuracy of post-processing algorithms run on meteorological model output. The wind field in coastal regions is influenced by complex physical processes associated with small-scale variations in terrain, and strong gradients in moisture, temperature, and surface roughness. The fundamental diurnal changes in the structure of the atmospheric boundary layer differ greatly from the land surface to the water surface. In part this is due to the fact that radiant energy arriving at the water surface is distributed over a large volume of water, while over land this energy is concentrated at the earth's surface. In addition, over the water surface persistent evaporation acts to lower the temperature of the air over the water surface in comparison to that over the land surface. Differences in the specific heats of water and soil also play a role, especially during the cooling cycle which begins in the evening hours. These effects lead to fundamental differences in heat fluxes between the two surfaces. As a result, the formation of a thermal internal boundary layer often takes place. Another result of these processes is that the stability regimes over water can differ greatly from those over land. Even the larger scale processes associated with these differences between the land boundary layer and marine boundary layer are difficult for a mesoscale model to capture.

Recent work by Titlow and McQueen (1999) has indicated that the current versions of the available operational meteorological models are incapable of producing reliable high-resolution wind forecasts during periods of weak synoptic-scale forcing. Although sea-breeze processes have been adequately simulated in research studies (e.g., Rao and Fuelberg 2000), operational prediction of small-scale processes such as the land-sea breeze circulation remains problematic for real-time NWP models available from NCEP. This is true even at high resolution (e.g., 4 km) grid spacing. Currently Titlow uses the output from these models as one component in his efforts to provide detailed wind field forecasts over the Chesapeake Bay. Any procedure that would make these meteorological

model output wind fields more useful to him and others like him would be of great benefit to recreational interests (e.g., sailing, fishing, and wind surfing), commercial interests (e.g., shipping and aviation), and environmental interests.

In the summer of 2001, NASA and the Defense Threat Reduction Agency (DTRA) sponsored a field experiment (The Chesapeake Bay Numerical Weather Prediction Model Experiment) over the Chesapeake Bay (see Figure 1) to collect data pertinent to the numerical modeling community. Data were collected over the period July 16 to July 31. These days were chosen in the hopes that weakly forced flow conditions would prevail for a good portion of this period. Unfortunately, only the period 21-23 July fully met that criterion. It was hoped that the data collected could be used to improve the ability of mesoscale models to forecast the state of the atmosphere over complex terrain when small scale processes dominate the flow regime, either by improving initial conditions or in the development of a post-processing technique that could be applied to meteorological model output. Limited data collection was continued into the summer of 2002. The criterion of weakly forced conditions was better met in 2002 than in 2001. This study will examine data from the 2002 period. During this period both observed data and MM5 (Penn State University/National Center for Atmospheric Research Mesoscale Model Version 5) output fields were available.

The research presented in this paper represents a novel approach to wind field modeling, analysis and spatial prediction.

The difficult challenge of modeling the spatial structure of wind fields over time can be overcome by using *separable processes*. A spatial-temporal field $Z(\mathbf{s}, t)$, where $\mathbf{s}$ represents space and t time, is *separable* if $\mathrm{Cov}\{Z(\mathbf{s}, t), Z(\mathbf{s}', t')\} = C_1(\mathbf{s}, \mathbf{s}')C_2(t, t')$ for some spatial covariance C_1 and temporal covariance C_2. This class of spatial-temporal processes offers enormous computational benefits, because the covariance matrix can be expressed as the Kronecker product of two smaller matrices that arise separately from the temporal and purely spatial processes, and then its determinant and inverse are easily determinable. Thus, separability is a desirable property for spatial-temporal processes, but it is usually a rather unrealistic assumption for large spatial-temporal domains, and there is little written about nonseparable models. What is novel about this paper is the introduction of new classes of space-time nonstationary and nonseparable families of covariance models. New fitting algorithms are developed to estimate the space-time covariance.

The true wind field (speed and direction) is a quantity that is not known. It is a function of a spatial-temporal trend term and a zero mean process, which has a nonseparable and non-stationary covariance that might change with location. In this research, the true wind is determined by

conditioning on the observed wind field at specified locations and on the wind fields derived from MM5, a widely used mesoscale meteorological model. The observed wind field at any particular location is treated as a function of the true (but unknown) wind and measurement error. The wind field from the numerical model is treated as function of a linear and multiplicative bias and a term which represents random deviations with respect to the true wind process.

A Bayesian approach is taken to providing information about the true wind field. To obtain the posterior predictive distribution of the true wind field given the observed and MM5 forecast wind fields, prior distributions must be identified for the set of parameters related to both the observed wind and the model forecast wind field as well as the spatial/temporal nature of the data sets. In addition, the likelihood must be specified. In order to to arrive at the posterior predictive distribution, a multi-stage Gibbs sampling approach is used to simulate values for the set of parameters from the posterior distribution of the parameter vector given the observed and the MM5 predicted wind fields.

This approach provides a representation of the wind field that is potentially more accurate than that from operational data assimilation systems. In a sense, this procedure can be considered to be a post-model run hierarchical Bayesian nudging procedure. This Bayesian modified model output field would provide a more accurate picture of the atmosphere for subsequent model runs. A similar approach was proposed by Best et al. (2000), who relate different spatially varying quantities to an underlying unobservable random field for a regression analysis of health and exposure data. In our method we also have an underlying unobservable process, but the statistical model we propose is novel. We present a new way to relate meteorological variables to an underlying process: in this case the true wind values. We also propose new models for nonseparable processes. Wikle et al. (2001) presented an approach to combining data from different sources to improve the prediction of wind fields. Wikle et al.'s approach is a conditional one in which all the spatial quantities are defined through a series of statistical conditional models. In their approach the output of the numerical models is treated as a prior process. We present here a simultaneous representation of the data and the output of numerical models in terms of the underlying truth. Our method is very different from Wikle et al.'s, since we do not treat the output of the numerical models as a prior process, but as another source of data. Therefore, we write the output of the models in terms of the underlying truth, taking into account the potential bias of the numerical models.

This paper is organized as follows. In Section 2 we present new classes of nonseparable and nonstationary models for space-time processes. In Section 3 we model the spatial-temporal trend using

a space-time dynamic model with varying coefficients. In Section 4 we describe the algorithm for wind field mapping. In Section 5 we apply the methods described in this paper to wind field data.

2 Modeling the spatial-temporal dependence structure

2.1 Spectral representation

A random field Z in $\mathbb{R}^d$ is called *weakly* stationary (or stationary), if it has finite second moments, its mean function is constant and it possesses an autocovariance function C, such that $C(\mathbf{x}-\mathbf{y}) = \text{cov}\{Z(\mathbf{x}), Z(\mathbf{y})\}$. If $C(h) = C_0(|h|)$ for some function C_0, then the process is called isotropic.
The spectral representation of a random process $Z(\mathbf{x})$ is always interpreted as its representation in the form of the superposition of sine and cosine waves of different frequencies $\boldsymbol{\omega}$. If Z is a stationary random field with autocovariance C, then we can represent the process in the form of the following Fourier-Stieltjes integral (see Yaglom (1987) for example):

$$Z(\mathbf{x}) = \int_{\mathbb{R}^2} \exp(i\mathbf{x}^T\boldsymbol{\omega}) dY(\boldsymbol{\omega}) \tag{1}$$

where the Y are random functions that have uncorrelated increments with complex symmetry except for the constraint, $dY(\boldsymbol{\omega}) = -dY^c(-\boldsymbol{\omega})$, needed to ensure $Z(\mathbf{x})$ is real-valued. Y^c denotes the conjugate of Y. Using the spectral representation of Z and proceeding formally,

$$C(\mathbf{x}) = \int_{\mathbb{R}^2} \exp(i\mathbf{x}^T\boldsymbol{\omega}) F(\mathbf{d}\boldsymbol{\omega}), \tag{2}$$

where the function F is a positive finite measure and is called the spectral measure or spectrum for Z. The spectral measure F is the mean square value of the process Y,

$$E\{|Y(\boldsymbol{\omega})|^2\} = F(\boldsymbol{\omega}).$$

If F has a density with respect to Lebesgue measure, it is the spectral density, f, which is the Fourier transform of the autocovariance function:

$$f(\boldsymbol{\omega}) = \frac{1}{(2\pi)^2} \int_{\mathbb{R}^2} \exp(-i\mathbf{x}^T\boldsymbol{\omega}) C(\mathbf{x}) d\mathbf{x}.$$

Each random process (not necessarily a stationary process) having a covariance function of the form (2), where F is a function of bounded variation, is *harmonizable*. Such a process is representable as the Fourier-Stieltjes integral (1), where Z is a random function whose spectral function coincides with F.

2.2 A general class of space-time covariance models

A class of nonseparable spatial-temporal models have been proposed by Cressie and Huang (JASA, 99), Gneiting (JASA, 02), and by Stein (2003). Here, we define a generalized class of nonstationary and nonseparable spatial-temporal covariance models. For this class, the spectral representation itself and the corresponding spectral distribution function (or spectral density) can change slowly in space and time. Let Z be a general space-time process, we use the following representation

$$Z(\mathbf{x},t) = \int_{\mathbb{R}^3} \exp(i\mathbf{x}^T\boldsymbol{\omega} + it\tau) dY_{\mathbf{x},\mathbf{t}}(\boldsymbol{\omega},\tau). \tag{3}$$

We are going to assume throughout this Section that the mean of the process is zero. We will define a model for the mean in Section 3. We capture the potential lack of stationarity by allowing the spectral process Y associated with Z to change in space and time. Other nonstationary approaches for spatial prediction have been proposed by Sampson and Guttorp (1992), Smith (1996), Haas (1995), Higdon et al. (1999), Wikle et al. (2001), Fuentes (2001) and (2002), Fuentes and Smith (2001), and Nychka et al. (2003) among others.

The general spectral representation proposed here (3) provides an ideal framework to model complex space-time dependent structures. Next, we discuss two flexible space-time covariance models that correspond to processes with this type of spectral representation.

2.2.1 Mixture of local spectrums (Spectral model)

A particular case of the general representation in (3) is when the lack of stationarity is explained by allowing the amplitude of the spectral process Y to be space-time dependent. This means

$$Z(\mathbf{x},t) = \int_{\mathbb{R}^3} \exp(i\mathbf{x}^T\boldsymbol{\omega} + it\tau)\phi_{\mathbf{x},\mathbf{t}}(\boldsymbol{\omega},\tau) dY_0(\boldsymbol{\omega},\tau) \tag{4}$$

where $\phi_{\mathbf{x},\mathbf{t}}(\boldsymbol{\omega},\tau)$ is an amplitude function (space-time dependent), and Y_0 is a Wiener process (space-time invariant), which satisfies the relation

$$E\left[Y_0(\boldsymbol{\omega},\tau)Y_0^c(\boldsymbol{\omega}',\tau')\right] = \delta(\boldsymbol{\omega}-\boldsymbol{\omega}')\delta(\tau-\tau')d\boldsymbol{\omega}'d\tau'$$

where δ is the delta Dirichlet function. This is a space-time version of the evolutionary spectrum presented by Priestley (1965). We assume the functions $\phi_{\mathbf{x},\mathbf{t}}(\boldsymbol{\omega},\tau)$ satisfy the condition

$$\int_{\mathbb{R}^3} |\phi_{\mathbf{x},\mathbf{t}}(\boldsymbol{\omega},\tau)|^2 d\boldsymbol{\omega}d\tau < \infty \tag{5}$$

for all $\mathbf{x}$ and t. The functions $\phi_{\mathbf{x},\mathbf{t}}(\boldsymbol{\omega},\tau)$ must also satisfy $\phi_{\mathbf{x},\mathbf{t}}(\boldsymbol{\omega},\tau) = -\phi^c_{\mathbf{x},\mathbf{t}}(\boldsymbol{\omega},\tau)$ to ensure $Z(\mathbf{x},t)$ is real-valued.

Then, it is easy to see that the covariance function, C, of the process $Z(\mathbf{x},t)$ is given by the formula

$$\begin{aligned}\mathrm{cov}\{Z(\mathbf{x}_1,t_1),Z(\mathbf{x}_2,t_2)\} &= C(\mathbf{x}_1,t_1;\mathbf{x}_2,t_2)\\ &= \int_{\mathbb{R}^3}\exp\{i(\mathbf{x}_1-\mathbf{x}_2)^T\boldsymbol{\omega})\}\exp\{i(t_1-t_2)^T\tau\}\phi_{\mathbf{x}_1,t_1}(\boldsymbol{\omega},\tau)\phi^c_{\mathbf{x}_2,t_2}(\boldsymbol{\omega},\tau)d\boldsymbol{\omega}d\tau\end{aligned} \tag{6}$$

In particular

$$\mathrm{var}\{Z(\mathbf{x},t)\} = C(\mathbf{x},t;,\mathbf{x},t) = \int_{\mathbb{R}^2}|\phi_{\mathbf{x},\mathbf{t}}(\boldsymbol{\omega},\tau)|^2 d\boldsymbol{\omega}d\tau \tag{7}$$

so that condition (5) is necessary for the variance of $Z(\mathbf{x},t)$ to be finite at all $\mathbf{x}$ and t, i.e. for the existence of a covariance function $C(\mathbf{x}_1,t_1;\mathbf{x}_2,t_2)$. The representation in (4) may be interpreted as a representation of the process Z in the form of a superposition of sinusoidal oscillations with different frequencies $\boldsymbol{\psi}=(\boldsymbol{\omega},\tau)$ and random amplitudes $\phi_{\mathbf{x},\mathbf{t}}(\boldsymbol{\omega},\tau)dY(\boldsymbol{\omega},\tau)$ varying over space, i.e. $Z(\mathbf{x},t)$ is a superposition of amplitude modulated random oscillations. According to this interpretation, (7) describes the distribution of the "total power" of the process $Z(\mathbf{x},t)$ at location $\mathbf{x}$ and time t over the frequencies $\boldsymbol{\psi}$, hence the contribution from the frequency $\boldsymbol{\psi}$ is $|\phi_{\mathbf{x},\mathbf{t}}(\boldsymbol{\omega},\tau)|^2 d(\boldsymbol{\omega})d\tau$. Therefore the function $F_{\mathbf{x},\mathbf{t}}(\boldsymbol{\omega},\tau)$ defined by the relation

$$dF_{\mathbf{x},\mathbf{t}}(\boldsymbol{\omega},\tau) = |\phi_{\mathbf{x},\mathbf{t}}(\boldsymbol{\omega},\tau)|^2 d\boldsymbol{\omega}d\tau \tag{8}$$

will be called the spatial spectral distribution function of the process Z, and $f_{\mathbf{x},\mathbf{t}}(\boldsymbol{\omega},\tau)=|\phi_{\mathbf{x},\mathbf{t}}(\boldsymbol{\omega},\tau)|^2$ is the spatial spectral density of Z.

There exist different representations of the form (3) for a spatial-temporal process Z, each representation is based on a different family of $\phi_{\mathbf{s}}(\boldsymbol{\psi})$ functions, where we write $\mathbf{s}=(\mathbf{x},\mathbf{t})$ and $\boldsymbol{\psi}=(\boldsymbol{\omega},\tau)$ to simplify the notation. This problem is similar to the selection of a basis for a vector space. Apart from that, it would not be physically meaningful to interpret $\boldsymbol{\psi}$ as the frequency in all cases. In the physical theory of oscillations the function $A_{\mathbf{s}}(\boldsymbol{\psi})=\phi_{\mathbf{s}}(\boldsymbol{\psi})\exp(i\mathbf{s}^T\boldsymbol{\psi})$ is said to describe the amplitude modulated oscillation of frequency $\boldsymbol{\psi}$ only if the "amplitude" $\phi_{\mathbf{s}}(\boldsymbol{\psi})$ is a slowly varying compared to $\exp\{i\mathbf{s}^T\boldsymbol{\psi}\}$ function, i.e. if the Fourier transform of $\phi_{\mathbf{s}}(\boldsymbol{\psi})$ as a function of $\mathbf{s}$ includes mainly frequencies much lower than $\boldsymbol{\psi}$. It is even often assumed that this transform must be concentrated in a neighborhood of zero frequency. We restrict the permissible variability of the function $\phi_{\mathbf{s}}(\boldsymbol{\psi})$ of $\mathbf{s}$ by considering only functions $\phi_{\mathbf{s}}(\boldsymbol{\psi})$ that admit a generalized Fourier representation

$$\phi_{\mathbf{s}}(\boldsymbol{\psi}) = \int_{\mathbb{R}^3} e^{i\mathbf{s}^T\boldsymbol{\sigma}}dH_{\boldsymbol{\psi}}(\boldsymbol{\sigma}) \tag{9}$$

with $|dH_{\boldsymbol{\psi}}(\boldsymbol{\sigma})|$ having its maximum at $\boldsymbol{\sigma}=\mathbf{0}$ for any fixed $\boldsymbol{\psi}$. This condition guarantees that the Fourier transform of $\phi_{\mathbf{s}}(\boldsymbol{\psi})$, as a function of $\mathbf{s}$, includes mainly frequencies much lower than any $\boldsymbol{\psi}$,

and it has been suggested by Priestley in the time series context. Since $\phi_{\mathbf{s}}(\boldsymbol{\psi})$ is a slowly varying function of space and time, it is clear that the process Z may be regarded as being "approximately jointly stationary" within subregions in our space-time domain D. If, however, we examine the behavior of Z within two subregions which are sufficiently far apart, we could find that although Z is practically stationary in both subregions, the spectral distribution function of the two "portions" of Z will, in general, be different (i.e., the spectral distribution of the power of Z varies on space and time). Since the functions $\phi_{\mathbf{s}}(\boldsymbol{\psi}) = 1$ clearly satisfy the conditions to be imposed on $\phi_{\mathbf{s}}(\boldsymbol{\psi})$, the representation (3) certainly includes all the spatial-temporal stationary processes having a finite variance. A particular case is when ϕ is a separable function of space and time, i.e.

$$\phi_{\mathbf{s}}(\boldsymbol{\psi}) = \phi_{\mathbf{x}}^{(1)}(\boldsymbol{\omega})\phi_{t}^{(2)}(\tau). \tag{10}$$

When ϕ is of the form (10) the spatial-temporal process is separable,

$$\begin{aligned}
&\mathrm{cov}\{Z(\mathbf{x}_1, t_1), Z(\mathbf{x}_2, t_2)\} \\
&\quad = \int_{\mathbb{R}^3} \exp\{i(\mathbf{x}_1 - \mathbf{x}_2)^T\boldsymbol{\omega})\}\exp\{i(t_1 - t_2)^T\tau\}\phi_{\mathbf{x_1}}^{(1)}(\boldsymbol{\omega})\phi_{t_1}^{(2)}(\tau)(\phi_{\mathbf{x_2}}^{(1)}(\boldsymbol{\omega}))^c(\phi_{t_2}^{(2)}(\tau))^c d\boldsymbol{\omega}d\tau \\
&\quad = \int_{\mathbb{R}^2} \exp\{i(\mathbf{x}_1 - \mathbf{x}_2)^T\boldsymbol{\omega})\}\phi_{\mathbf{x_1}}^{(1)}(\boldsymbol{\omega})(\phi_{\mathbf{x_2}}^{(1)})^c(\boldsymbol{\omega})d\boldsymbol{\omega}\int_{\mathbb{R}^1} \exp\{i(t_1 - t_2)^T\tau\}\phi_{t_1}^{(2)}(\tau)(\phi_{t_2}^{(2)}(\tau))^c d\tau \\
&\quad = C^{(1)}(\mathbf{x}_1, \mathbf{x}_2)C^{(2)}(t_1, t_2).
\end{aligned} \tag{11}$$

where $C^{(1)}$ and $C^{(2)}$ are spatial and temporal covariance functions.

We propose a more general model for ϕ that has the separable model in (10) as a particular case . We model ϕ as a mixture of local spectral (amplitude) functions,

$$\phi_{\mathbf{s}}(\boldsymbol{\psi}) = \sum_{i=1}^{k} K(\mathbf{s} - \mathbf{s}_i)\phi_{\mathbf{s}_i}(\boldsymbol{\psi}) \tag{12}$$

where each $\phi_{\mathbf{s}_i}(\boldsymbol{\psi})$ function explains the spatial-temporal structure of Z in a neighborhood of $\mathbf{s_i}$. Locally (in a neighborhood of $\mathbf{s_i}$), we propose the following general nonseparable parametric model for $\phi_{\mathbf{s}_i}$, that has a separable model as a particular case,

$$\phi_{\mathbf{s}_i}(\boldsymbol{\omega}, \nu) = \gamma_i(\alpha_i^2\beta_i^2 + \beta_i^2\|\boldsymbol{\omega}\|^2 + \alpha_i^2|\tau|^2 + \epsilon_i\|\boldsymbol{\omega}\|^2|\tau|^2)^{-(\nu_i + d)/2} \tag{13}$$

The parameter α_i^{-1} explains the rate of decay of the spatial correlation component. For the temporal correlation, the rate of decay is explained by β_i^{-1}, and γ_i is a scale parameter. The parameter $\nu_i > 0$ measures the degree of smoothness of the process Z at $\mathbf{s}_i$, the higher the value of ν_i the smoother Z would be. The Fourier transform of $\phi_{\mathbf{s}_i}(\boldsymbol{\omega}, \nu)$ is a Matérn-type covariance function. If $\epsilon_i = 0$ we

have a 3-d Matérn type model with different spatial and temporal ranges, which takes into account the change in units from the spatial to the temporal domain. If $\epsilon_i = 1$ we have a separable model,

$$\phi_{\mathbf{s}_i}(\boldsymbol{\psi}) = \gamma_i(\alpha_i^2 + \|\boldsymbol{\omega}\|^2)^{-(\nu_i+d)/2}(\beta_i^2 + |\tau|^2)^{-(\nu_i+d)/2}. \tag{14}$$

Then, the corresponding (local) covariance is separable (as in (11)).

2.2.2 Mixture of local space-time models (Spatial domain)

Another particular case of the general representation in (3) is when the spectral process $Y_{\mathbf{x},\mathbf{t}}(\boldsymbol{\omega}, \tau)$ is modeled as a mixture of (orthogonal) local stationary spectral processes Y_i for $i = 1, \ldots, k$ that explain the space-time dependence structure in subregions of stationarity $S_1, \ldots, S_k$,

$$Y_{\mathbf{x},\mathbf{t}}(\boldsymbol{\omega}, \tau) = \sum_{i=1}^{k} K(\mathbf{s} - \mathbf{s}_i)Y_i(\boldsymbol{\omega}, \tau) \tag{15}$$

where each Y_i explains the spatial-temporal structure of Z in a subregion of stationarity S_i. Thus, we can write the process Z in terms of orthogonal processes Z_i, for $i = 1, \ldots, k$

$$Z(\mathbf{x}, \mathbf{t}) = \sum_{i=1}^{k} K(\mathbf{s} - \mathbf{s}_i)Z_i(\mathbf{x}, \mathbf{t}) \tag{16}$$

where for $i = 1, \ldots, k$, Z_i is the space-time stationary process associated with Y_i.
The corresponding covariance function for a process Z with the spectrum given by (15) is

$$\text{cov}\{Z(\mathbf{x}_1, t_1), Z(\mathbf{x}_2, t_2)\} = \sum_{i=1}^{k} K(\mathbf{s}_1 - \mathbf{s}_i)K(\mathbf{s}_2 - \mathbf{s}_i)C_i(\mathbf{x}_1 - \mathbf{x}_2, t_1 - t_2) \tag{17}$$

where $\mathbf{s}_i = (\mathbf{x}_i, t_i)$, and each C_i is a stationary covariance (corresponding to the spectral process Y_i) that explains the space-time dependency in a subregion of stationarity S_i.
We propose the following parametric model for C_i,

$$C_i(\mathbf{x}, t) = \frac{\sigma_i}{2^{\nu_i-1}\Gamma(\nu_i)}(2\nu_i^{1/2}\|(\mathbf{x}, \beta t)\|/\rho_i)^{\nu_i}\mathcal{K}_{\nu_i}(2\nu_i^{1/2}\|(\mathbf{x}, \beta_i t)\|/\rho_i), \tag{18}$$

where $\mathcal{K}_{\nu_i}$ is a modified Bessel function and the covariance vector parameter, $\boldsymbol{\theta}_i = (\nu_i, \sigma_i, \rho_i, \beta_i)$, changes from subregion to subregion to explain the lack of stationarity. The parameter ρ_i measures how the correlation decays with distance; generally this parameter is called the *range*. The parameter σ_i is the variance of the random field, i.e., $\sigma_i = \text{var}(Z_i(\mathbf{x}, t))$, where the covariance parameter σ_i is usually referred to as the *sill*. The parameter ν_i measures the degree of smoothness of the local stationary process Z_i (as in (14). The parameter β_i is a scale factor to take into account the change

of units between the spatial and temporal domains. This parametric model for C_i corresponds to a 3-d Matérn type covariance with an extra parameter (β_i) that can be interpreted as a conversion factor between the units in the space and time domains. A more general model for C_i would be given by the Fourier transform of $f_{\mathbf{s}_i}$ in (13). When $\epsilon_i = 0$, the model for C_i in (18) is just a particular case of (13).

The representation for a general space-time process given in (4), with ϕ defined in (12), also corresponds to a mixture of space-time stationary processes

$$Z(\mathbf{x}, \mathbf{t}) = \sum_{i=1}^{k} K(\mathbf{s} - \mathbf{s}_i) Z_i^*(\mathbf{x}, \mathbf{t}) \tag{19}$$

where each Z_i^* is a stationary process with covariance C_i, and K is the kernel function in (12). The difference between this representation and (16) is that the local stationary processes in (19) are correlated to each other, and in (12) they are orthogonal. The cross-covariance between Z_i^* and Z_j^* is given by

$$\text{cov}\{Z_i^*(\mathbf{x}_1, t_1), Z_j^*(\mathbf{x}_2, t_2)\} = \int_{\mathbb{R}^3} \exp\{i(\mathbf{x}_1 - \mathbf{x}_2)^T \boldsymbol{\omega})\} \exp\{i(t_1 - t_2)^T \tau\} f_i^{1/2}(\boldsymbol{\omega}, \tau) f_j^{1/2}(\boldsymbol{\omega}, \tau) d\boldsymbol{\omega} d\tau \tag{20}$$

where the functions $f_i = \phi_i^2$ and $f_j = \phi_j^2$ are the square of the amplitude functions.

3 Spatial-temporal Trend

In the previous section of this manuscript we have introduced some new models for the spatial-temporal covariance/spectrum. In this section we present spatial-temporal models for the large scale structure or trend using covariates with dynamic coefficients.

We represent the large scale structure of Z using a space-time dynamic statistical model:

$$Z(s,t) = \sum_{i}^{k} \beta_i(s,t) f_i(s,t) + \varepsilon(s,t), \tag{21}$$

where $\{f_i\}_i$ are k covariates (e.g. sine and cosines and geographic data) of interest with coefficients β_i that vary in space and time. The residual term $\varepsilon(s,t)$ is a space-time correlated error that explains the spatial-temporal short scale structure.

We model the dynamic coefficients β_i using a hierarchical model in terms of an overall time component $\gamma_{i,t}$ and a space-time process $\gamma_i(s,t)$,

$$\beta_i(s,t) = \gamma_{i,t} + \gamma_i(s,t)$$

$$\gamma_{i,t} = \gamma_{i,t-1} + u(t)$$

$$\gamma_i(s,t) = \gamma_i(s,t-1) + \eta(s,t)$$

η and u are independent white noise processes. We estimate the parameters in the model with their posterior distribution (given the data D), i.e. $P(\beta|D)$.

4 Wind mapping combining measurements and model output

In our statistical approach to wind field mapping, which combines observed data and model output (Fuentes and Raftery, 2001), we do not consider the measurements at the monitoring stations to be the "truth" because of measurement error. Thus, we assume there is an underlying (unobserved) field $Z(\mathbf{x},t)$, where $Z(\mathbf{x},t)$ measures the "true" meteorological variable at location $\mathbf{x}$ and time t. At station $\mathbf{x}$, we make an observation $\hat{Z}(\mathbf{x},t)$ corresponding to the observation at this station at time t, and we assume that

$$\hat{Z}(\mathbf{x},t) = Z(\mathbf{x},t) + e(\mathbf{x},t), \tag{22}$$

where $e(\mathbf{x},t) \sim N(0,\sigma_e^2)$ represents the measurement error (nugget) at location $\mathbf{x}$.

The true underlying process Z is a spatial process with a nonstationary and nonseparable covariance,

$$Z(\mathbf{x},t) = \mu(\mathbf{x},t) + \varepsilon(\mathbf{x},t), \tag{23}$$

where $Z(\mathbf{x},t)$ has a space-time trend, $\mu(\mathbf{x},t)$, that is modeled as a function of some meteorological and geographic covariates using model (21).

We assume that $Z(\mathbf{x},t)$ has zero-mean correlated errors $\varepsilon(\mathbf{x},t)$. The process $\varepsilon(\mathbf{x},t)$ has a nonstationary and nonseparable covariance with parameter vector $\boldsymbol{\theta}$ that might change with location.

We could model the output of the meteorological models as follows:

$$\tilde{Z}(\mathbf{x},t) = a(\mathbf{x},t) + b(\mathbf{x},t)Z(\mathbf{x},t) + \delta(\mathbf{x}). \tag{24}$$

Here, the parameter function $a(\mathbf{x},t)$ measures the additive bias of the weather metereological models at location $\mathbf{x}$ and time t, and the parameter function $b(\mathbf{x},t)$ accounts for the multiplicative bias in the metereological models. The process $\delta(\mathbf{x},t) \sim N(0,\sigma_\delta^2)$ explains the random deviation at location $\mathbf{x}$ with respect to the underlying true process $Z(\mathbf{x},t)$.

Wind field mapping

We seek to obtain more reliable wind field spatial predictions by combining model output with observations. Thus, for the prediction of wind field we simulate values of Z from the posterior

predictive distribution of the true underlying wind process given the model output and the observations:

$$P(Z|\hat{Z}, \tilde{Z}). \tag{25}$$

This is a calibrated wind prediction. It could also be considered a data assimilation approach in the sense that we are using the data to improve the wind forecast, but in contrast with the traditional approach of perturbing the model inputs and assimilating data using Kalman-Filter methods, we perturb the output using the data to produce a calibrated model output.

5 Application

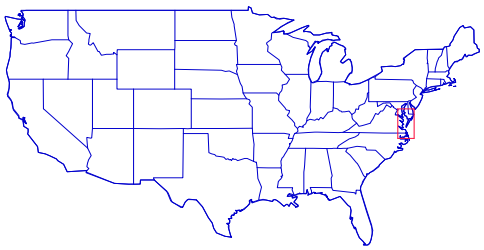

Figure 1: *The box shows our study domain in the Chesapeake Bay region.*

The red box in Figure 1 shows our study domain in the Chesapeake Bay region. Forecasting the wind field over the Bay is of long-standing interest because it is composed of many features that are spatially and temporally complex in nature. The goal of our study is to understand the spatial-temporal structure of wind fields over the Bay and to obtain more reliable wind field predictions by combining model output with observations. The analysis for wind speed on July 21, 2002 is presented here.

5.1 Description of the data

Both observed and MM5 00Z model output wind fields were used in this study. The observed data were collected by an independent suite of meteorological stations owned by Weatherflow, Inc (see Fig. 2) and provided by Jay Titlow of Weatherflow, Inc. The MM5 data were furnished by John McHenry at Baron's Advanced Meteorological Systems. The observed wind data were collected at the locations shown in Figure 2. The anemometers were location from 9 to 18 m above ground level, depending on the location. Adjustment of the wind speed values to the standard 10 m height was accomplished using Monin-Obukhov similarity theory (Arya, 2001). This adjustment had little affect on the wind speed values given the small distances involved. The MM5 model output

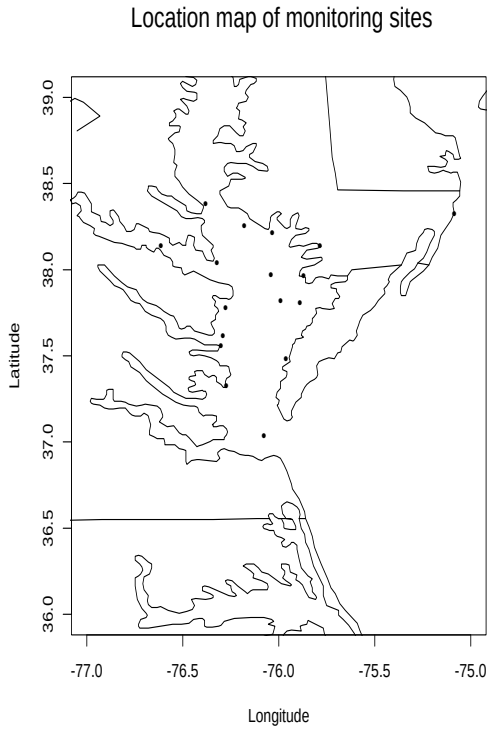

Figure 2: *The location map of monitoring sites.*

fields were generated using a 15-km Arakawa C grid (see Figure 3) This grid spacing was selected because it is similar to the finest mesh produced by operational models run at the National Centers for Environmental Prediction (NCEP), and based on discussions with Jay Titlow at Weatherflow, Inc. Winds from the lowest model layer were used after adjustment to the 10m level. In this analysis, data from 21 July 2002 have been examined in detail for the full 24-hr period. The complicated flow patterns over the region during this time are evident in Figure 4. The arrows

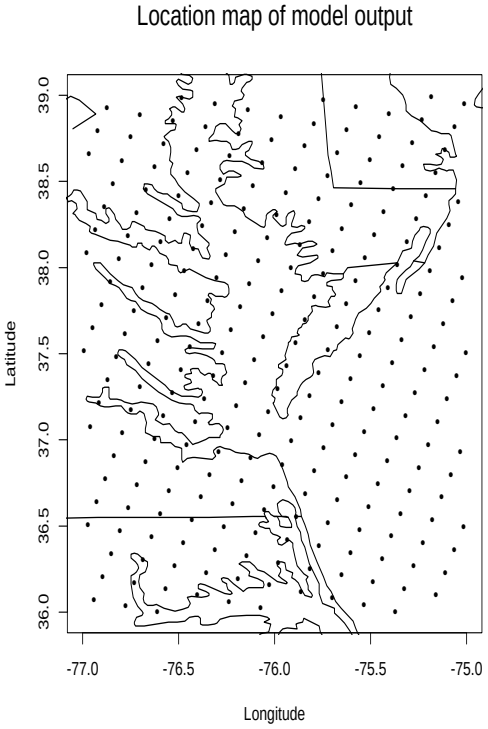

Figure 3: *Grid for MM5 output.*

indicate the direction from which the winds are coming, while the length of the stem indicates wind speed in meters per second. The plots were done at 3-hr intervals. A streamline (streamlines are lines that are everywhere tangent to the instantaneous wind vector) analysis (not shown) of the flow fields shows alternating areas of confluence (areas where the streamlines tend to come together) and diffluence (areas where the streamlines tend to spread apart). Confluence may or may not be associated with mass convergence, while diffluence may or may not be associated with mass divergence depending on how the wind speed changes in these zones (Petterssen, 1956).

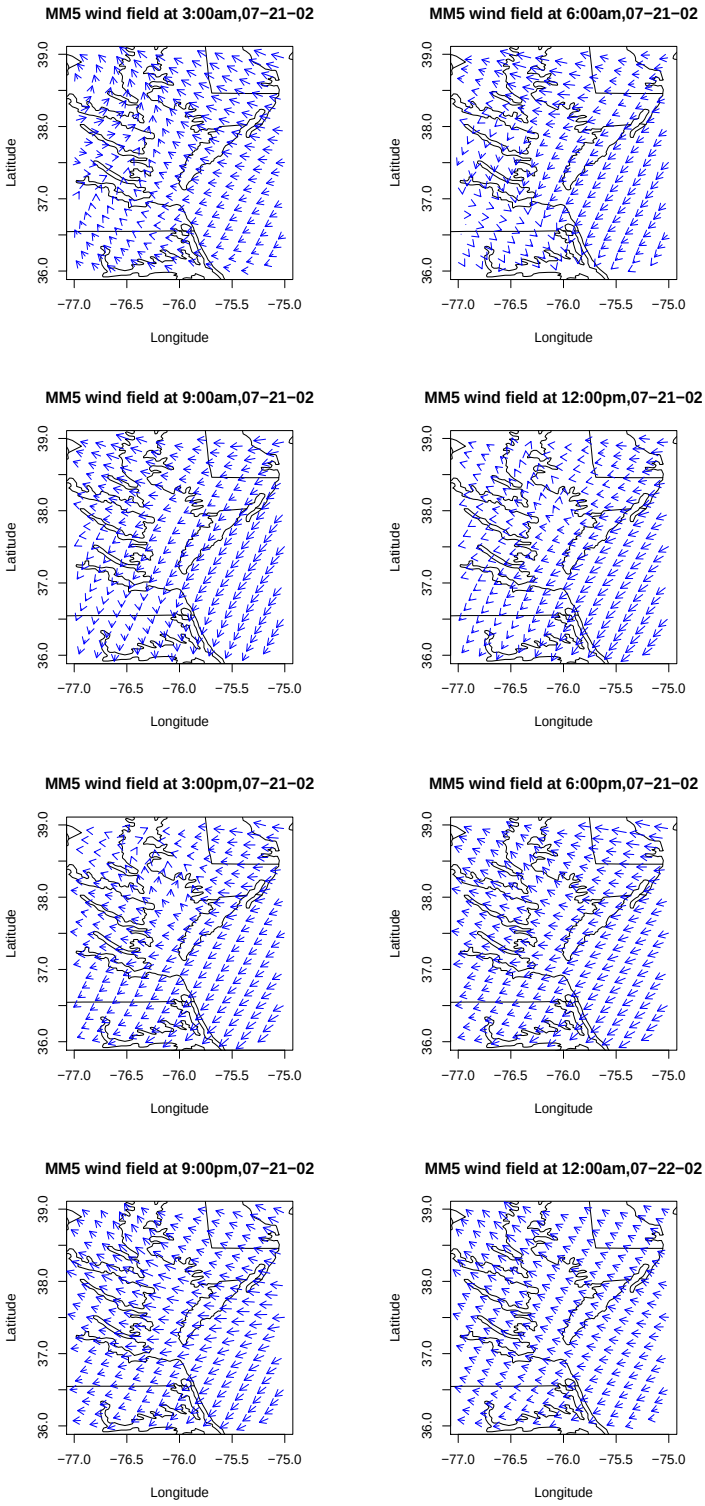

Figure 4: *Wind field maps, showing wind direction and speed.*

An easterly (winds from the east, southeast and northeast) wind component tends to dominate over the region for this time period. The 3AM plot clearly shows an area of confluence on the west side of the Bay. At 6AM this area of confluence has been replaced by an area of diffluence over the center of the Bay. Diffluence seems to persist over the Bay for the rest of the period. There is little evidence in these plots to suggest that MM5 was capturing the sea breeze circulation, which observations show to be present.

5.2 The nonstationarity for wind fields

As a first empirical attempt to dealing with the nonstationarity inherent in these kinds of environmental data, we divided the spatial domain into two broad categories: land and water. From an atmospheric boundary layer standpoint, this partition appears to be a reasonable way to approach the problem of nonstationarity. Using the u wind component, v wind component and wind speed from the model output at noon on July 21, 2002, the K-means cluster procedure was used to further subdivide these two regions to help identify domains of stationarity. We iterated this process until the AIC criteria suggested that there was no significant improvement in the estimation of the covariance parameters for the wind speed anomalies (wind value at each location minus the mean over time at that location) using the theoretical covariance model presented in Section 5.4. The optimal number of clusters suggested by the AIC criteria was five. The five subregions are shown in Figure 5. This final regional arrangement of clusters appears reasonable considering atmospheric and oceanic processes that are occurring in the boundary layer on this day. It is reasonable to assume that there will be some changes in the configuration of these regions as time passes and the boundary layer structure changes. For the purposes of this work, we assumed that the changes were negligible.

5.3 Spatial-temporal trend

A spatial-temporal trend is fitted using the the space-time dynamic model proposed in Section 3, which has two components. One is the overall temporal trend for the process Z (the truth), and it doesn't change with location. The other part is the temporal variation that changes with location. The covariates used here are sine and cosine functions with respect to two different periods (1/frequency): 24 hours and 12 hours, which capture the diurnal and half-diurnal cycles. These two components of the spatial-temporal trend are shown in the Figure 6. This trend is fitted using a Bayesian hierarchical framework. The parameters are estimated using the mean of the posterior

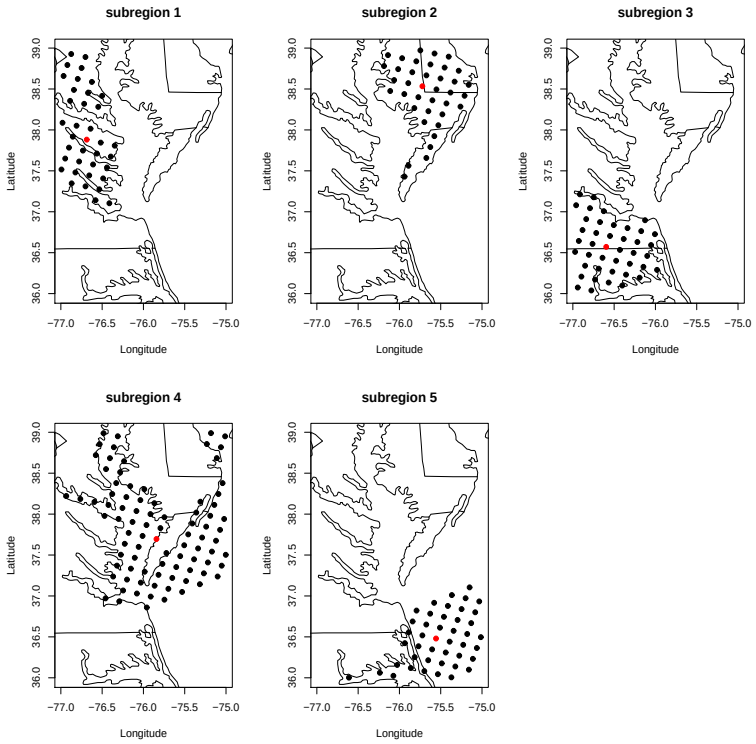

Figure 5: *Subregions of stationarity.*

distribution. Figure 6 (a) shows the overall wind speed trend over time. From Figure 6 (a) it appears that from a time standpoint the highest wind speeds over the region as a whole occur near sunset, while the minimum wind speeds on that day occur near sunrise. Figure 6 (b) shows the temporal variation for each subregion. The anomalies for subregions 1 and 3 are generally negative over time, while for subregions 4 and 5 they are generally positive. Subregion 2 starts out positive but then becomes negative. The large positive values in subregion 5 indicate that the wind speeds in that subregion are higher than the average during the mid-day hours. The large mid-day negative values for subregion 1 indicate that the wind speeds are lower than average during the mid-day hours in that subregion.

In the next stage of our hierarchical design we estimate the covariance.

5.4 Spatial-temporal covariance structure

Empirical covariance analyses

We start with an empirical analysis of the covariance structure. We draw empirical covariance graphs for each subregion for the wind speed anomalies (wind value at each location minus the mean

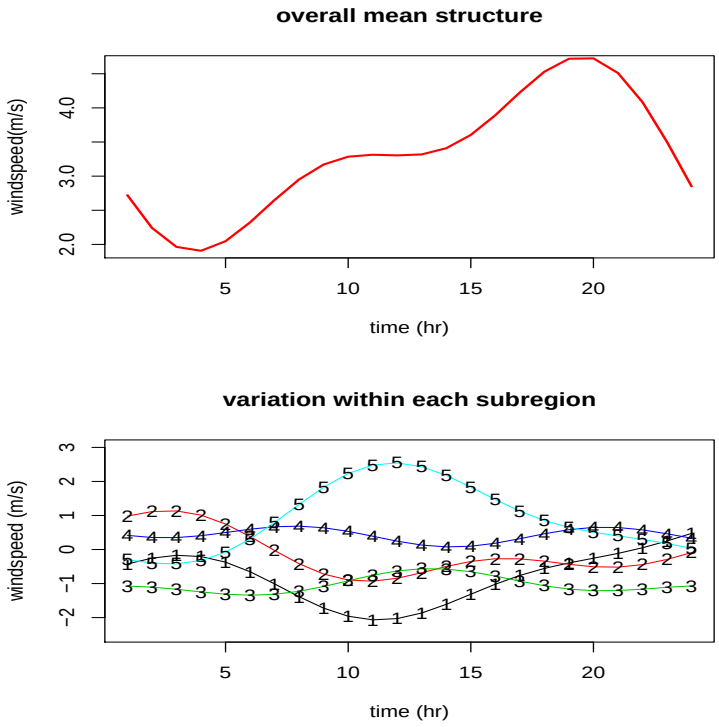

Figure 6: *Spatial-temporal trend for wind speed. Top graph (a): overall temporal trend. Bottom graph (b): mean temporal variation for each subregion.*

over time at that particular location). Figure 7 clearly shows ridges in the empirical covariances for subregions 1, 2, 3 and 5. These type of ridges appear in separable covariance structures. On the other hand, the empirical covariance plot for subregion 4 appears to be smoother, there does not seem to be a ridge effect, suggesting a non-separable covariance structure. The tests for stationarity, separability and isotropy proposed by Fuentes (2003) within each subregion were performed. Stationarity was found to hold within each subregion. Separability was found to hold within all subregions except for subregion 4. The results from the formal tests agree with the empirical covariance analyses.

Theoretical covariance model

We model the covariance of Z using model (17) proposed in Section 2.2.2. with 5 subregions of stationarity (as in Figure 5). For subregion 4 we use the nonseparable model (18). For the separable spatial-temporal covariances in the other subregions we use Matérn models for the spatial covariance and exponential models for the temporal covariance. We fit the parameters for the spatial-temporal covariance of Z using a Bayesian framework. In our covariance model, we allowed for geometric

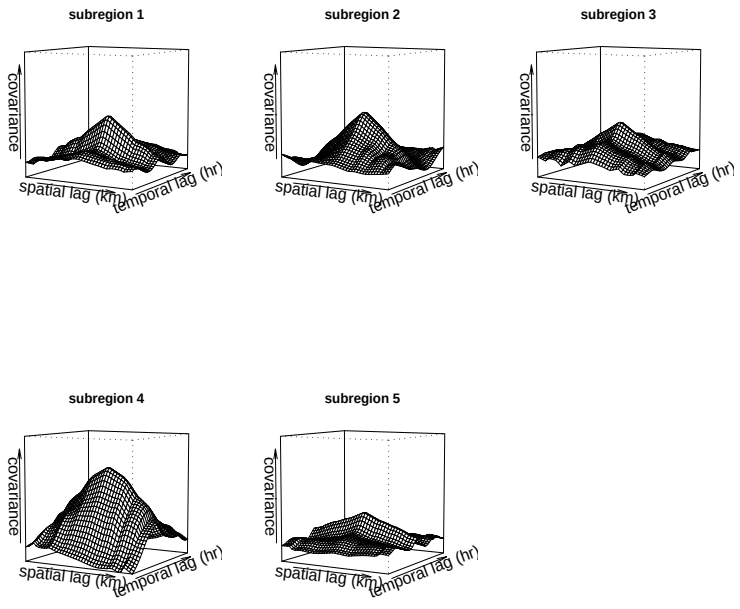

Figure 7: *Space-time empirical covariance.*

anisotropy. Subregion 1 and subregion 5 seemed to be anisotropic, which means that the spatial covariance depended not only on distance but also direction. A linear transformation was used to transform the coordinates (x, y). The new coordinates are $(x', y') = RT(x, y)^T$, where R is a rotation matrix and T is a shrinking matrix. R and T are defined as follows:

$$R = \begin{pmatrix} \cos A & \sin A \\ -\sin A & \cos A \end{pmatrix} \text{ and } T = \begin{pmatrix} 1 & 0 \\ 0 & \frac{1}{r} \end{pmatrix},$$

A describes the angle of rotation and r is used to stretch the coordinates. These anisotropy parameters are estimated with their posterior distribution as well as the other covariance parameters. The prior distributions that we specified for the sill, the temporal range and the spatial range are $IG(, 2)$. The prior distributions for the anisotropy parameters (A and r), the smoothness parameter (ν)) for the Matérn class and the scale parameter (scale factor β) in the non-separable case, are uniform distributions; with support $(0, 2\pi)$ for A, and support $(0, \infty)$ for the other parameters.
The posterior densities for the sill parameter of each subregion are shown in Figure 8. The difference in the subregions (see Figure 5) are also reflected in the posterior distributions for the sill parameter. The largest mean of the posterior distributions was found for subregion 4, which encompasses

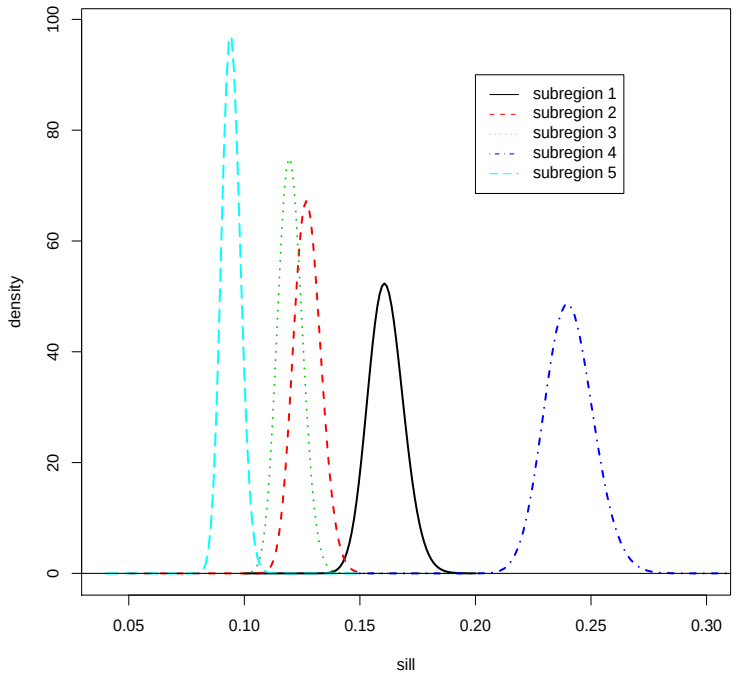

Figure 8: *Posterior distribution for the sill parameter.*

a large variety of land and water surfaces. These large variations in the surface roughness characteristics would contribute to large variations in wind speed across the region. In addition, a major contribution to the wind speed variations can be attributed to stability differences which exist between land and water surfaces due in large part to the differential heating experienced by these surfaces. Subregion 4 is the least homogeneous of the five subregions. The second most spatially diverse subregion is subregion 1. Its sill value reflects this diversity. In addition, the significant differences in the sill parameter is evidence for the nonstationarity over the spatial domain.

The posterior distribution for the spatial range shown in Figure 9 indicates that subregion 5 has the highest posterior mean. Again, this result is consistent with the nature of the subregion. One would expect strong spatial continuity in this subregion. The posterior mean is lower for the other subregions, where the spatial continuity is weak.

The spatial-temporal covariance model (18) is used for subregion 4, which is non-separable. Figure 10 shows the posterior density of the scale parameter. The scale parameter takes into account the change of units between the spatial and temporal domains.

The spatial smoothness parameter (Figure 11) does not change much from subregion to subregion,

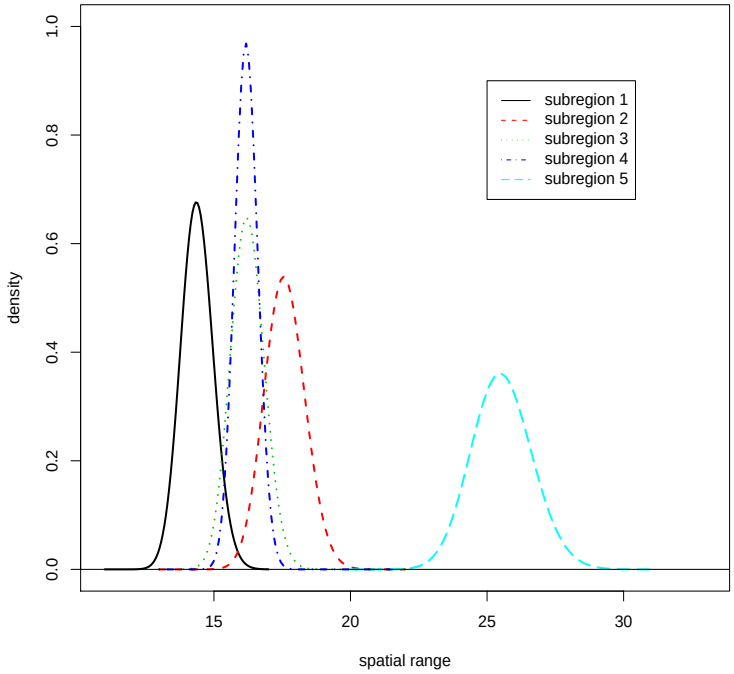

Figure 9: *Posterior distribution for the spatial range.*

the mean of the posterior distribution for this parameter is always between .5 and 1.5.

The posterior means of the covariance parameters are listed below:

Process	sill	spatial range	temporal range	smoothness	A	R	scale
subregion 1	0.1615	14.44	2.02	0.70	2.78	1.11	
subregion 2	0.1275	17.62	1.64	0.88			
subregion 3	0.1200	16.24	1.92	0.99			
subregion 4	0.3073	16.61		1.42			13.24
subregion 5	0.0944	25.64	1.73	0.58	1.18	1.17	

The estimated Bayesian covariance plots are shown in Figure 12.

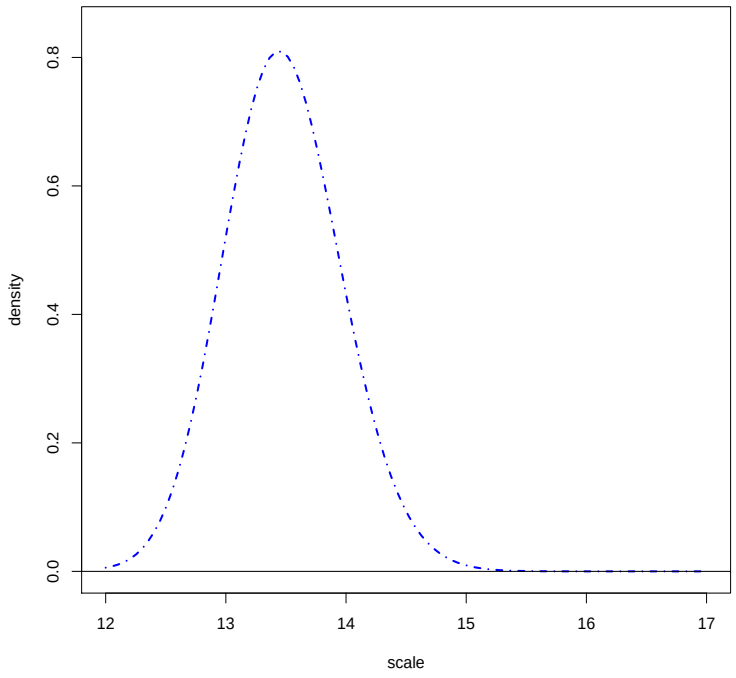

Figure 10: *Posterior distribution for the scale parameter.*

5.5 Wind field mapping

The original MM5 output wind speed map is shown in Figure 13. The colors in the image represent wind speeds from MM5, and the value on top of the image is the observed wind speed. Figure 13 indicates that there is a substantial difference between the MM5 output and the observed data. For the prediction of wind fields we simulate values of the wind speed from the posterior predictive distribution of the true underlying wind process given the model output and the observations. Figure 14 shows an improved wind map obtained by combining model output and observed wind data.

In Figure 14, the color of the background is the mean of posterior predictive distribution. The improved map agrees better with the observed data. In order to quantify this improvement we calculated the $MSE = \frac{1}{n}\sum_{i=1}^{n}(\hat{r}_i - r_{oi})^2$, where r_{oi} is the observed wind speed at location i, $\hat{r}_i$ is the predicted wind speed at location i (without using r_{oi}) and n is the number of observations. The MSE for the MM5 forecast is 10.32 and with our approach we reduced it to 2.45.

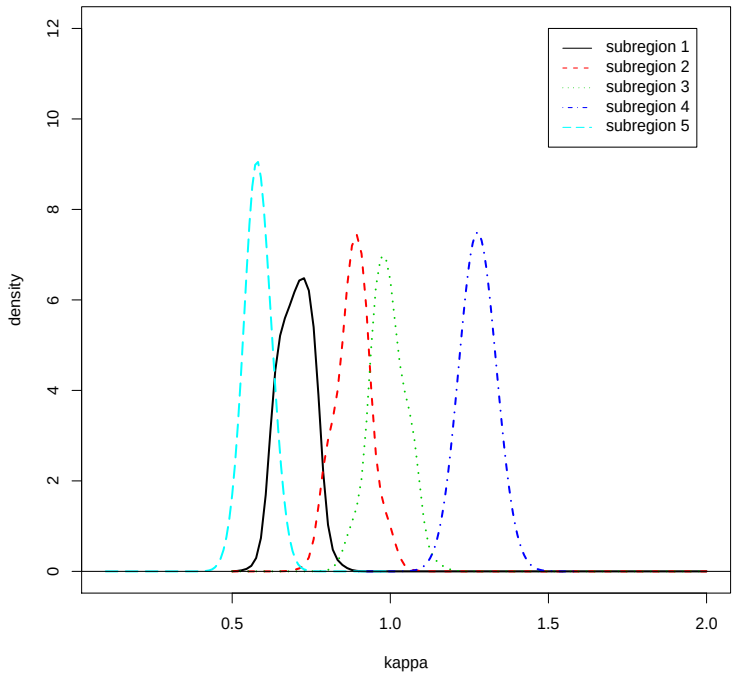

Figure 11: *Posterior for smoothness parameter.*

6 Discussion

In this paper we introduce new statistical models for spatial prediction of wind fields using different sources of data. We combine spatial data by relating the spatially varying variables to an underlying unobservable true wind field process and we predict this latent process. This is different from the traditional geostatistical approaches of cokriging or kriging with external drift (KED) for spatial interpolation with auxiliary covariates, as used by Phillips et al (1997), and Davis et al. (2000). In cokriging or KED we write the data in a regression model as a function of some covariates. Therefore, if the observed data and the output of numerical models exhibit different spatial resolution or are observed at different locations, we could not write directly the observed data as a function of the output of numerical models or vice versa. In this paper we overcome that problem by writing each source of information in terms of the truth, without assuming we observe it. The general statistical models introduced in this paper for spatial temporal processes allow for lack of stationarity, isotropy and they do not assume separability.

From a meteorological viewpoint, this technique could be used to improve the assimilation of the surface wind field observations into the meteorological model initial field. In addition, it could

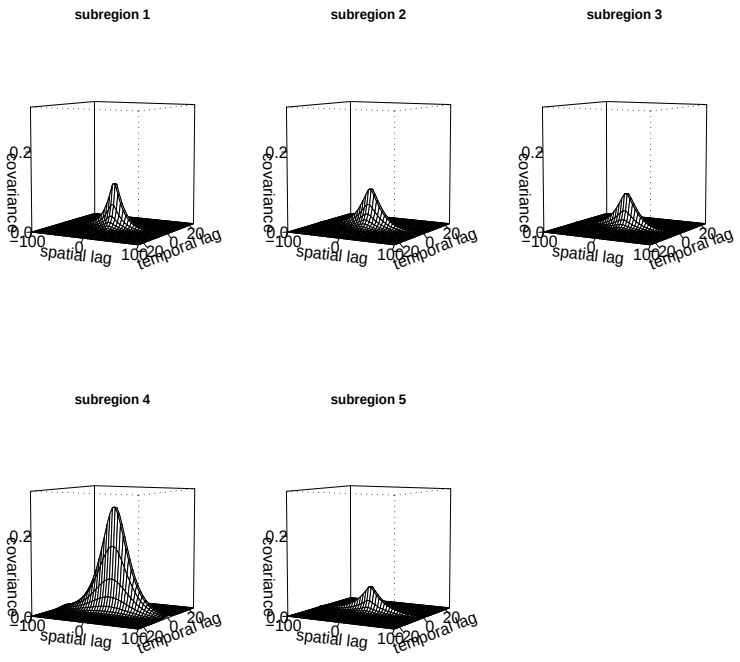

Figure 12: *Space-time covariance with parameters estimated with the mean of their posterior distributions.*

serve as a post-processing algorithm which would be run on meteorological model output fields. The meteorological community has been working on the data assimilation problem for many years. This research has produced some very sophisticated methodologies. For a current review of this literature see Kalnay (2003). The work by Daley (1991) and Talagrand (1997) should also be consulted.

Kalnay (2003) points out that early in the history of the the development of numerical weather prediction techniques it was found that a complete first guess estimate of the state of the atmosphere was required in addition to the traditional set of observations. The first guess field should be the meteorologist's best estimate of the state of the atmosphere before incorporating the observations. In a statistical sense, this is similar to the specification of a prior in Bayesian analysis. Currently short-range forecasts serve as the first guess field in what has come to be called the "analysis cycle." According to Kalnay, the analysis cycle is an intermittent data assimilation procedure which typically uses a 6-hr cycle performed four times a day. In areas where there are many observing sites, the observed data have the most influence on the model initial field, while in areas where

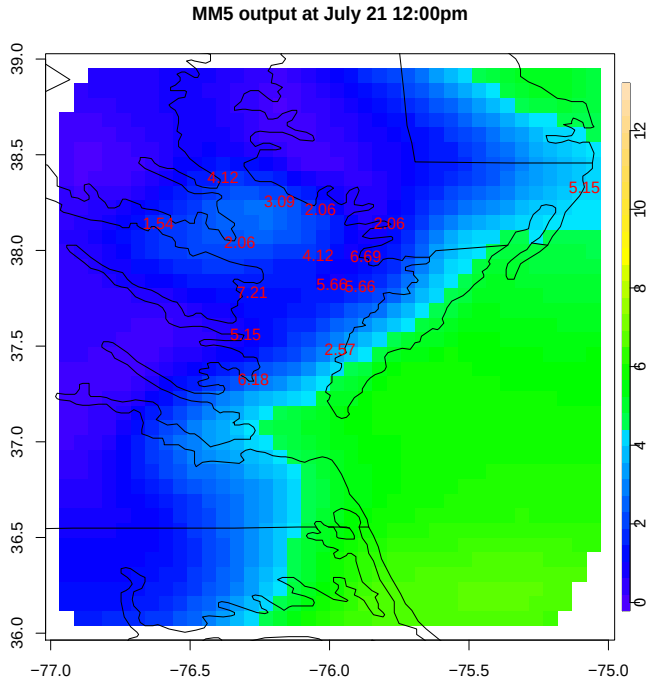

Figure 13: *Original MM5 output wind speed.*

observational data are scarce the model first guess field is important since it can build on the observational data from data rich areas. The procedure outlined in this paper provides a powerful technique for combining the first guess field with the available observations.

The improvement obtained in the mean square error when the meteorological model output and the observed data are combined is very good. However, these results are based on a very limited time period and have not been compared to other currently available methods. While the techniques presented in this paper have great promise, both further testing on larger data sets and comparison with exisitng techniques will show their true worth.

The technique itself does hold some promise for use in the forecasting mode. As noted in the paper, the subregions were derived based on the noon data for one day. Even under weakly forced synoptic flow regimes, these subregions of stationary can be expected to shift from hour to hour. One alternative might be to group hours together based on the diurnal restructuring of the atmospheric boundary layer. Using this technique, the subregimes may be more stable from day to day. In addition the day-to-day stability of the covariance function should be examined. Under weakly forced flow conditions these functions may show enough stabiltiy to be useful in the forecast

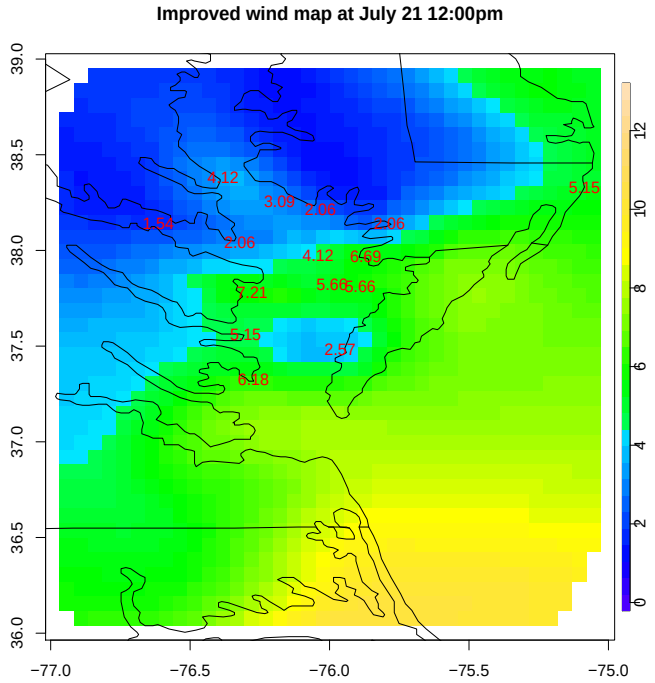

Figure 14: *Improved wind speed by combing data*

mode.

References

Arya, S. Pal. (2001). *Introduction to Micrometeorology.* New York: Academic Press.

Best, N. G., Ickstadt, K. and Wolpert, R. L. (2000). Spatial poisson regression for health and exposure data measured at disparate resolutions. *Journal of the American Statistical Association*, **95**, 1076-1088.

Chen, L., Fuentes, M, and Davis, J.M. 2003. Bayesian hierarchical spatio-temporal models for wind prediction. Proceeding of the 2003 Joint Statistical Meetings, San Francisco, August 3-7.

Cressie, N. and Huang, H.–C. (1999). Classes of nonseparable, spatio-temporal stationary covariance functions. *Journal of the American Statistical Association,* **94**, 1330-1340.

Daley, R. 1991. Atmospheric data analysis. New York: Cambridge Uinversity Press.

Davis, J. M., Nychka, D., and Bailey, B. (2000). A comparison of regional oxidant model (ROM) output with observed ozone data. *Atmospheric Environment,* **34**, 2413-1423.

Fuentes, M. (2001). A new high frequency kriging approach for nonstationary environmental processes. *Envirometrics,* **12**, 469-483.

Fuentes, M. (2002). Spectral methods for nonstationary spatial processes.*Biometrika,* **89** 197-210.

Fuentes, M. (2003). Testing for separability of spatial-temporal covariance functions. Tech. report at North Carolina State University, Institute of Statistics Mimeo Series #2545.

Fuentes, M. and Smith, R. (2001). A new class of nonstationary models. Tech. report at North Carolina State University, Institute of Statistics Mimeo Series #2534.

Fuentes, M. and Raftery, A. E. (2002). A Bayesian approach to combine disparate spatial data. Tech. report at North Carolina State University, Institute of Statistics Mimeo Series #2538.

Gneiting, T. (2002). Nonseparable, stationary covariance functions for space-time data, *JASA*, **97**, 590-600.

Haas, T.C. (1995), Local prediction of a spatio-temporal process with an application to wet sulfate deposition. *Journal of the American Statistical Association*, **90**, 1189–1199.

Higdon, D., Swall, J. and Kern, J. (1999), Non-stationary spatial modeling. In *Bayesian Statistics 6*, eds. J.M. Bernardo *et al.*, Oxford University Press, pp. 761–768.

Kalnay, E. 2003. Atmospheric modeling, data assimilation, and predictability. New York: Cambridge University Press.

Matérn, B. (1960). *Spatial Variation.* Meddelanden från Statens Skogsforskningsinstitut, **49**, No. 5. Almaenna Foerlaget, Stockholm. Second edition 1986), Springer-Verlag, Berlin.

Nyhcka, D., Wikle, C. and Royle, A. (2003). Multiresolution models for nonstationary spatial covariance functions. *Statistical Modelling,* **2**, 315-331.

Petterssen, S. (1956). *Weather Analysis and Forecasting: Volume I, Motion and motion systems.* New York: McGraw-Hill.

Phillips, D. L., Lee, H. E., Herstrom, A. A., Hogsett, W. E., and Tingey, D. T. (1997). Use Of auxiliary data for spatial interpolation of ozone exposure in southeastern forests. *Environmetrics,* **8**, 43-61.

Priestley, M. B. (1965). Evolutionary spectral and non-stationary processes. *Journal of the Royal Statistical Society. Series B.* **27**, 204-237.

Rao, P. A., and H. E. Fuelberg, (2000). An investigation of convection behind the Cape Canaveral sea-breeze front. *Mon. Wea. Rev.* **128**, 3437-3458.

Sampson, P.D. and Guttorp, P. (1992). Nonparametric estimation of nonstationary spatial covariance structure. *Journal of the American Statistical Association,* **87**, 108-119.

Sampson, P.D. and Guttorp, P. (1998). Operational Evaluation of Air Quality Models. Proceedings of a Novartis Foundation Symposium on Environmental Statistics.

Smith, R.L. (1996), Estimating nonstationary spatial correlations. Preprint, University of North Carolina.

Stein, M.L. (2003). Space-time covariance functions. Tech. Report, University of Chicago.

Talagrand, O. 1997. Assimilation of observations, an introduction. J. Met. Soc. Japan. 75:191-209.

Titlow, J.K. and J.T. McQueen, (1999). On the Use of a Coastal Mesonet as a Tool for Mesoscale Model Evaluation. Third Conference on Coastal Atmospheric Prediction and Processes, New Orleans, LA, American Meteorological Society, November 3-5, 1999.

Wikle, C. K., Milliff, R. F., Nychka, D. and Berliner, M. (2001). Spatiotemporal Hierarchical Bayesian Modeling: Tropical Ocean Surface Winds. *Journal of the American Statistical Association,* **95** 1076-1987.

Yaglom, A. M. (1962). *An introduction to the theory of stationary random functions.* Prentice-Hall, NJ.